

Electronic structure, first and second order physical properties of MPS_4 : a theoretical study

TAHAR DAHAME^{1*}, BACHIR BENTRIA¹, HOUDA FARAOUN², ALI BENGHIA¹, A.H. RESHAK^{3,4}

¹Laboratoire de Physique des Matériaux, Amar Telidji University of Laghouat, Algeria

²Département de Physique, Abou Bakr Belkaid University of Tlemcen, Algeria

³New Technologies - Research Center, University of West Bohemia, Univerzitni 8, 306 14 Pilsen, Czech Republic

⁴Center of Excellence Geopolymer and Green Technology, School of Material Engineering, University Malaysia Perlis, 01007 Kangar, Perlis, Malaysia

We have calculated the electronic structure and physical properties of metal thiophosphate compounds $InPS_4$ and $AlPS_4$ by means of pseudopotential density functional theory (DFT) coupled with the modern theory of polarization. The targeted physical properties are first and second order optical properties as well as elastic, piezoelectric and electro-optic coefficients. Furthermore, population analysis is presented in order to evaluate the covalent-ionic character of the constituent bonds. The calculated elastic constants, refractive indices and second order optical coefficients of $InPS_4$ are in good agreement with experimental values. With the absence of any theoretical or experimental physical properties of $AlPS_4$, we predict that this compound has high piezoelectric coefficients with $d_{14} = -73.82$ pm/V, $d_{25} = -10.96$ pm/V and $d_{36} = 28.19$ pm/V.

Keywords: *metal thiophosphate; DFT; optical, elastic, piezoelectric, electro-optic properties*

© Wrocław University of Technology.

1. Introduction

Modern technological developments require more research on the physical properties of materials such as optical and mechanical properties, which are closely linked to crystalline and electronic structures of the materials. In a recent survey [1], it has been pointed out that chalcogenide materials are potential candidates for nonlinear optical applications. They possess high nonlinear optical (NLO) coefficients and large transparency domains extending in the middle-IR region above 5 μm . Furthermore, chalcogenide materials show rich structural and compositional diversity and excellent IR transparency [2].

In the MPS_4 ($M = \text{Al, B, Ga and In}$) family, $InPS_4$ and $AlPS_4$ crystallize in a non-centrosymmetric structure and hence, they are good candidates for piezoelectric and electro-optic devices. Furthermore, they are anisotropic which

makes them also valuable candidates for second order NLO applications. Their large band gaps, of the order of 3.5 eV, enables them to have good optical transparency in the visible and ultraviolet region of the spectrum without suffering from the double photon absorption in NLO processes [3]. Their crystallographic structure belongs to the so called twice defective chalcopyrite [4]. Several groups of researchers have made these compounds the object of their experimental studies. However, to the authors' knowledge, no theoretical calculations of electronic band structure or elastic, piezoelectric, electro-optic and NLO properties of the compounds have been reported.

In 1970, the synthesis and growth of small single crystals of $InPS_4$ from vapor phase by iodine transport have been reported [5]. The crystallographic structure was determined by Carpentier et al. [6]. It belongs to the non-centrosymmetric space group I-4 with $a = 5.60$ Å and $c = 9.02$ Å. It is a three dimensional structure made of corner-connected $[PS_4]$ and $[InS_4]$ tetrahedrons (Fig. 1a).

*E-mail: dahametahar@yahoo.fr

Bridenbaugh [7] reported that InPS_4 has relatively large nonlinear second order optical coefficients. In 1975, Bubenzer *et al.* [8] synthesized crystals of InPS_4 up to 10 mm using improved vapor growth procedure. They also measured their piezoelectric constants by a non-resonant dynamic method and found that this compound has good coefficients with $d_{36} = 21.0$ pC/N. Huard *et al.* [9] synthesized large InPS_4 single crystals with good optical transparency and used Brillouin scattering method to measure their elastic constants. A complete survey of the elastic and optical properties of InPS_4 was reported by Jantz *et al.* [10]. They also evaluated the elastic tensor and found similar results to those reported in the literature [9]. In addition, they reported dispersion curves of the ordinary and extraordinary refraction indices in the entire transparency range of the investigated compound and found a birefringence of the order of 0.04. Furthermore, they measured the second order NLO coefficients and found $d_{31} = 36$ pm/V and $d_{36} = 28$ pm/V. On the other hand, in 1993, Bolcatto *et al.* [11] used tight-binding method to calculate the electronic structures of the MPS_4 ($M = \text{B}, \text{Al}, \text{Ga},$ and In) thiophosphate family. In 2000, Lavrentyev *et al.* [12], investigated both experimentally and theoretically X-ray absorption near edge structure (XANES) of K-absorption spectra of P and S atoms in InPS_4 and in 2003 they focused their research on the electronic structure and chemical bonding in InPS_4 compound together with Tl_3PS_4 and $\text{Sn}_2\text{P}_2\text{S}_6$ [13]. They presented the partial electronic density of states from the experimental measurements using X-ray spectroscopy and theoretical quantum mechanical calculations, using ab-initio multiple scattering FEFF8 code. The same group in 2006 presented their results on the influence of pressure on the birefringence of ZnS , CuGaS_2 and InPS_4 compounds using the modified method of augmented plane waves and the code WIEN2k [14]. As far as AlPS_4 is concerned, no experimental or theoretical study has been reported except its crystal structure [11]. This study revealed that this compound crystallizes in the orthorhombic non-centrosymmetric space group $P222$ with the following cell parameters: $a = 5.61$ Å, $b = 5.67$ Å, $c = 9.05$ Å. AlPS_4 crystal structure consists of

edge-connected $[\text{AlS}_4]$ and $[\text{PS}_4]$ forming helicoidal chains along x and y axis as shown Fig. 1b. These chains are linked together by weak Van der Waals interactions.

The aim of this work is the theoretical calculation of electronic structure and physical properties of aluminum and indium thiophosphates by means of DFT and modern theory of polarization.

The remaining part of this paper is organized as follows: after this Introduction, Section 2 gives the computational details. Section 3 presents the calculated results and thorough discussions on the structural, elastic and optical properties of the materials. A brief summary and conclusion are presented in Section 4.

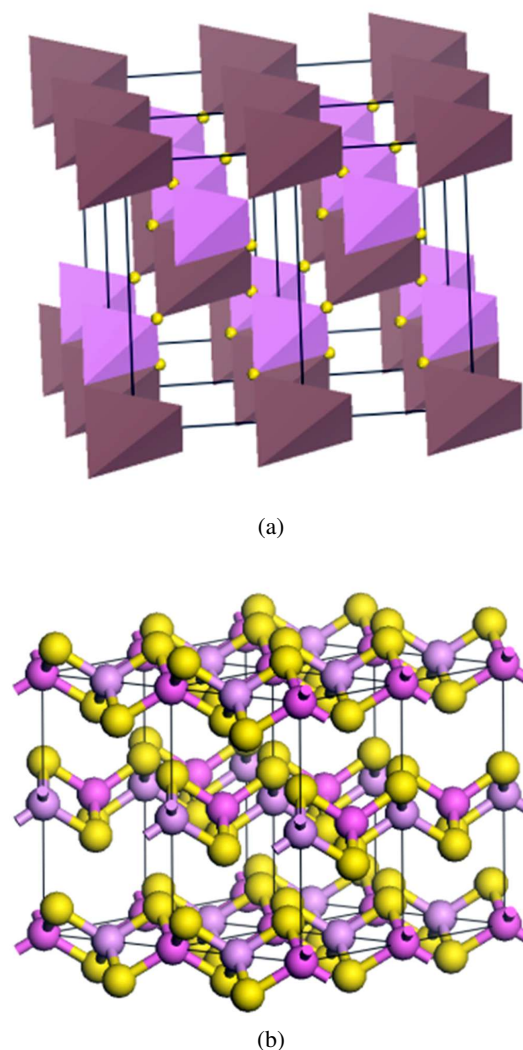


Fig. 1. Multi cell ($2 \times 2 \times 1$) (a) InPS_4 and (b) AlPS_4 .

2. Computational

The electronic structure, linear optical properties and elastic constants were calculated using the pseudopotential plane wave method, within density functional theory (DFT) as implemented in CASTEP computer code [15]. The generalized gradient approximation of Perdew-Burke-Ernzerhof (GGA) and local density approximation of Ceperley-Alder (LDA) were used as functional for exchange and correlation effects [16]. Ultra-soft pseudopotentials (USP) [17] were used with the following valence electronic configurations In (4d¹⁰ 5s² 5p¹), Al (3s² 3p¹), P (3s² 3p³), and S (3s² 3p⁴). In the elementary cells of the compounds the atomic positions are: In (0, 1/2, 3/4), P (0, 0, 0) for InPS₄ and Al (0, 0, 0), (1/2, 0, 1/2), P (0, 1/2, 0), (0, 0, 1/2) for AIPs₄. These atomic positions are not affected by the optimization because they are fixed by symmetry, however, it was necessary to relax the position of sulphur atoms in both compounds because of its general position (x, y, z).

The second order optical susceptibilities, piezoelectric and electro-optic coefficients were calculated within the framework of modern theory of polarization and density-functional perturbation theory DFPT as implemented in the open-source ABINIT code package [18, 19]. This theory has been shown to give successful description of the dielectric and piezoelectric properties of a wide range of materials in which electronic correlation is not too strong [20–22]. These calculations were carried out using Troullier-Martins norm-conserving pseudopotentials [23]. The exchange-correlation effects were treated within the (LDA) approximation [24] and Perdew-Wang 92 functional parameterizations [25]. For the crystal structure relaxation, electronic structure and all physical properties calculations, the convergence has been reached for both codes with an energy tolerance of 10⁻⁶ eV with E_{cut} = 600 eV and a 6 × 6 × 4 mesh grid for Brillouin zone sampling.

2.1. Linear optical properties

Linear optical properties described in this work are the absorption coefficient, refractive index and

dielectric constant. All these quantities are presented as a function of frequency of the electromagnetic wave that propagates through the crystal. The most important optical property of a material is the complex dielectric constant ϵ . The CASTEP code can calculate its imaginary part $\epsilon_2(\omega)$, using the following relation [26]:

$$\epsilon_2(\omega) = \frac{2e^2\pi}{\Omega\epsilon_0} \sum^{k,v,c} |\langle \psi_k^c | \vec{u} \cdot \vec{r} | \psi_k^v \rangle|^2 \delta(E_k^c - E_k^v - E) \quad (1)$$

where \vec{u} is the vector defining the polarization of the incident electric field, \vec{r} is the position operator, ψ_k^c and ψ_k^v represent the valence band and the conduction band states in which the direct transitions are possible, $E_k^c - E_k^v = \hbar\omega$ is the transition energy, ϵ_0 is the dielectric constant of free space, e is the electronic charge, Ω is the volume of unit cell and the integral is over the first Brillouin zone (BZ). The real and imaginary parts are linked by the Kramers-Kronig relation [27].

The other optical constants such as refractive index $n(\omega)$ and extinction coefficient $k(\omega)$ can be derived from the dielectric function using the relations:

$$\begin{aligned} \epsilon_1(\omega) &= n^2(\omega) - k^2(\omega) \\ \epsilon_2(\omega) &= 2n(\omega) \cdot k(\omega) \end{aligned} \quad (2)$$

2.2. Nonlinear optical properties

In the Nunes and Vanderbilt formalism [28], the total energy of the electronic system perturbed by the electric field is a functional of the Wannier functions. It is given by the following relation [29, 30]:

$$E(W_n, \vec{E}) = E_0(W_n) - \Omega_0 \cdot \vec{E} \cdot \vec{P} \quad (3)$$

where E is the total energy of the system. E_0 is the energy of Kohn-Sham of the fundamental state, Ω_0 is the volume of cell, \vec{P} is the macroscopic polarization, W_n is the Wannier function and \vec{E} is the electric field. The second term on the right depends explicitly on polarization. It is known as “energy of polarization” and noted as:

$$E_{pol} = -\Omega_0 \cdot \vec{E} \cdot \vec{P} \quad (4)$$

The term $\vec{E} \cdot \vec{P}$ acts as an external potential as well as the ionic potential; it is linear with the electric field and depends only on it. One can admit that the electric field plays the part of a perturbation. The second order dielectric susceptibility is calculated from the third order derivative of the energy of polarization with respect to electric field components [31]. Using the Voigt contracted notation:

$$d_{ij} = \frac{1}{2} \chi_{ij}^{(2)} \quad (5)$$

the tetragonal and orthorhombic (P222) crystal systems have four ($d_{14}, d_{15}, d_{31}, d_{36}$) and three (d_{14}, d_{15}, d_{36}) independent non-zero elements, respectively.

The electro-optic coefficients r_{ijk} characterize the linear electro-optical effect i.e. when the variation of refractive index is linearly proportional to the applied static or low frequency electric field. It is also known as the Pockels effect. These coefficients result from the electronic r_{ijk}^{el} and ionic r_{ijk}^{ion} contributions plus the contribution due to the opposite piezoelectric effect r_{ijk}^{piezo} [32]. There are four independent non-zero electro-optic elements ($r_{31}, r_{41}, r_{51}, r_{63}$) for tetragonal I-4 class crystals and three elements (r_{41}, r_{52}, r_{63}) for orthorhombic P222 class crystals.

2.3. Elastic properties

Elastic properties of a material are very important because they describe its response to an applied stress, or conversely the stress required to maintain a given deformation, and they are related to various physical phenomena, such as transmission of acoustic and thermal waves through the material.

Properties such as the bulk modulus (response to an isotropic compression), Poisson ratio, Lamé constants, and so forth may be computed from the values of elastic stiffness constants C_{ij} . Those constants are the relationships that determine the deformations produced by a given stress acting on a particular material. In tetragonal and orthorhombic crystal systems, the elastic tensor contains 7 ($C_{11}, C_{33}, C_{44}, C_{66}, C_{12}, C_{13}, C_{16}$) and 9 ($C_{11}, C_{22}, C_{33}, C_{44}, C_{55}, C_{66}, C_{12}, C_{13}, C_{23}$) independent

elements, respectively. For small elastic deformations ϵ_i along the direction i of the crystal, its potential energy has the form:

$$U_p = \frac{1}{2} \sum_{i,j} C_{ij} \epsilon_i \epsilon_j \quad (6)$$

and the stability condition is to have a determinant $[C_{ij}] > 0$. This condition results in the following stability relations: for tetragonal and orthorhombic system, respectively:

$$\begin{aligned} C_{ii} &> 0 (i = 1, 3, 4, 6) & (7) \\ C_{11} - C_{12} &> 0 \\ C_{11} + C_{33} - 2C_{13} &> 0 \\ 2C_{11} + C_{33} + 2C_{12} + 4C_{13} &> 0 \end{aligned}$$

$$\begin{aligned} C_{ii} &> 0 (i = 1 \text{ to } 6) & (8) \\ \sum_{i \neq j=1}^3 C_{ii} + 2C_{ij} &> 0 \\ C_{ii} + C_{jj} - 2C_{ij} &> 0 (i \neq j = 1, 2, 3) \end{aligned}$$

Several mechanical properties can be calculated through these coefficients, most important are: bulk B and shear G modulus, from which one can calculate the elastic λ and Young's E modulus, and Poisson's ratio ν [33].

2.4. Piezoelectric coefficients

From the response function capabilities of ABINIT, it is possible to estimate the piezoelectric coefficients d_{ij} by calculating the second derivatives of the total energy (2DTE) with respect to electric fields, and Cartesian strains [19]. In this method strains are treated as perturbations. The piezoelectric tensor, contains 3×6 elements. The total number of independent piezoelectric tensor members is determined by the point group of the material. In tetragonal and orthorhombic crystals systems, the matrix of piezoelectric tensor d contains four ($d_{14}, d_{15}, d_{31}, d_{36}$) and 3 (d_{14}, d_{15}, d_{36}) non zero elements, respectively; they have the same form and number of independent constants as non-linear optical tensor [34].

3. Results and discussion

3.1. Electronic structure

Full structure relaxation was carried out for both compounds for which the Hellman-Feynman forces acting on sulphur atom passed from few eV/Å prior to relaxation to lower than 10^{-3} eV/Å after the process. The calculated lattice parameters and atomic positions of sulphur atom in InPS₄ and AlPS₄ are presented in Table 1. Compared to the experimental values the calculated cell parameters are on average 0.83 % underestimated by the LDA and 6.92 % overestimated by the GGA. It should be noted here that the calculated a and b cell parameters of AlPS₄ have almost the same values which makes us think that its crystalline structure is tetragonal instead of the orthorhombic one. Our theoretical calculations also show a significant increase of c cell parameter of this compound.

The calculated energy band structures, total and partial density of states of InPS₄ and AlPS₄ are presented in Fig. 2. From these figures, one can draw several important remarks concerning the electronic properties of the two materials. Both compounds have indirect wide band gap: 2.535 eV for InPS₄ (M to Γ) and 2.706 eV for AlPS₄ (Y to S). Certainly these values are underestimated compared to the experimental ones, as in the case of InPS₄ which has an experimental gap of 3.44 eV [12]. This is a known failure of DFT attributed to the fact that this theory treats the ground state only and to the discontinuity in the exchange-correlation potential [16]. Furthermore, we notice an appreciable similarity between the band structures and density of states of our compounds. This has been much expected because of the presence of [PS₄]³⁻ and [MS₄]³⁺ tetrahedrons in both compounds. The valence bands of the materials are dominated by the contribution of p states of sulfur with a large contribution of p states of phosphorus and s states of the metal in the lower subband around -5 eV. The conduction band of the compounds is dominated by p electron states of phosphorus and sulfur and s and p states of the metal atoms. Furthermore, the d states of indium are localized around -14 eV and have no contribution

to the valence or conduction bands. They are expected to play no role in the optical properties of InPS₄.

We also carried out Mulliken population analysis that reflects the nature of bond between two atoms. It has a value ranging between 0 and 1. The tendency towards 0 indicates a dominant ionic character whereas the tendency towards the unity indicates the domination of covalent character. The intermediate interval shows a mixing character and a negative value indicates that the bond does not exist.

The results of Mulliken population analysis for both the compounds are presented in Table 2. These data indicate the existence of two types of mixed bonds in each compound. The P-S bonds are slightly skewed towards the covalent character whereas the M-S bonds have a rather ionic nature. The sign of ΔZ in Table 3 informs us on the donor or acceptor role played by each element in the compound. These results reveal a donor character of phosphorus and an acceptor character of sulfur atoms in both the compounds. The metal atoms are donors with higher activity of aluminum over indium. We also notice the absence of indium d electrons activity in donor-acceptor character.

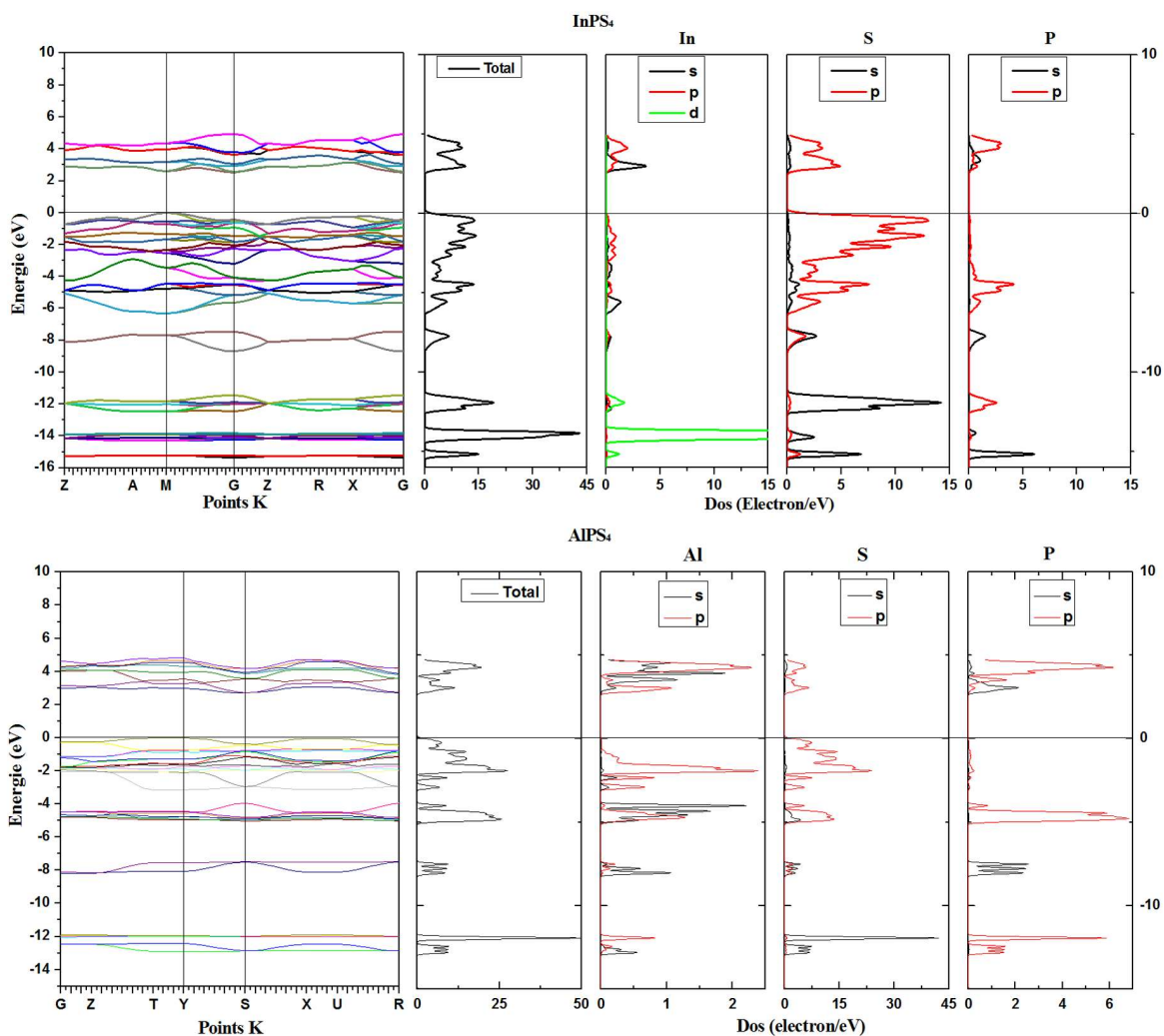
3.2. Linear optical properties

Graphs in Fig. 3 present the calculated real and imaginary parts of the complex dielectric constant $\epsilon(\omega) = \epsilon_1(\omega) + i\epsilon_2(\omega)$ the refractive index $n(\omega)$ and the absorption coefficient $\eta(\omega)$. These quantities are plotted along the electric field polarization directions $\langle 1 0 0 \rangle$, $\langle 0 1 0 \rangle$ and $\langle 0 0 1 \rangle$.

We can also follow the electronic transition from the valence band to the conduction band through the variations of imaginary part of $\epsilon(\omega)$ which presents several peaks. There are three essential peaks in the imaginary part $\epsilon_2^{001}(\omega)$ of InPS₄. The first one, A at 3.40 eV, corresponds to transitions from S 3p (VB) to In 5s and S 3p (CB). The next peak, B at 5.77 eV, is mainly due to transitions from S 3p (VB) to s and p states of the three elements in the CB. The third peak at 7.70 eV is due to the electronic transitions from S 3p and P 3p (VB) to In 5s, S 3p and P 3s of the CB. In case

Table 1. Structural parameters of relaxed lattice and sulphur coordinates.

	InPS ₄					AlPS ₄			
	Abinit (LDA)	Castep (LDA)	Castep (GGA)	Exp. [11] [5]		Abinit (LDA)	Castep (LDA)	Castep (GGA)	Exp. [11]
a [Å]	5.521	5.554	5.802	5.623	5.60	5.554	5.585	5.700	5.61
b [Å]	5.521	5.554	5.802	5.623	5.60	5.613	5.582	5.702	5.67
c [Å]	8.895	8.789	9.193	9.058	9.02	8.960	8.899	11.567	9.05
x	0.3110	0.3114	0.3068	0.3057	[11]	0.2159	0.2148	0.1988	0.200
						0.7736	0.7757	0.7778	0.740
y	0.2496	0.2461	0.2289	0.2389	[11]	0.2749	0.2768	0.2779	0.260
						0.7908	0.7907	0.8013	0.800
z	0.1286	0.1294	0.1327	0.1302	[11]	0.1206	0.1204	0.1000	0.125
						0.6248	0.6242	0.6003	0.630

Fig. 2. Band structures, total and partial Dos of InPS₄ and AlPS₄.

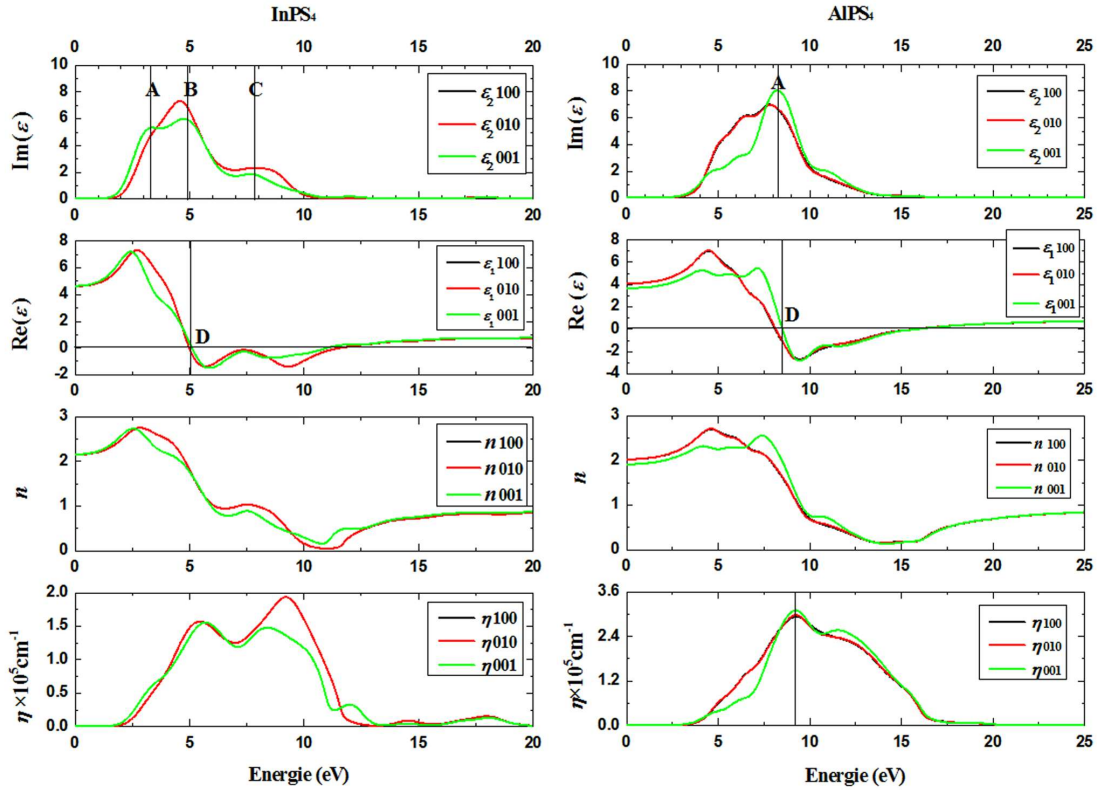
Fig. 3. Linear optical properties of InPS₄ and AIPs₄.

Table 2. Mulliken population analysis.

InPS ₄				AIPs ₄			
Bond Population	Bond lengths [Å]			Bond Population	Bond lengths [Å]		
	This work	Exp. [11]			This work	Exp. [11]	
P–S	0.56	2.045	2.53	P–S	0.55	2.056	2.1
In–S	0.43	2.534	2.47	Al–S	0.47	2.266	2.1
In–P	–	3.701	3.60	Al–P	–63.00	2.851	2.8

of AIPs₄ we notice a dominant peak at 8.27 eV which mainly corresponds to transitions from 3p states of sulfur and phosphorus to s and p states of three constituent elements in the CB. It should be noted that in the previous discussion only vertical interband transitions have been taken into consideration, since many direct and indirect electronic transitions may occur with an energy corresponding to the same peak.

We can also see similarities and differences between $\epsilon^{100}(\omega)$ and $\epsilon^{001}(\omega)$. The similarities are as follows: for low frequencies, which

correspond to energies less than band gap energy ($E_g(\text{InPS}_4) = 2.33$ eV, $E_g(\text{AIPs}_4) = 2.70$ eV), $\epsilon_2^{100}(\omega)$ and $\epsilon_2^{001}(\omega)$ are negligible and the material behaves as a transparent dielectric. The energy absorption range starts from E_g and extends up to about 15 eV. In this range the material behaves like a dielectric absorber for energies lower than the energy of resonance, i.e. 5.13 eV (InPS₄), 8.53 eV (AIPs₄) which corresponds to point D in Fig. 3, and as metallic absorber in the rest of the range, where it becomes reflective. Beyond this range ($E > 15$ eV) the material becomes transparent with the dielectric constant tending to 1 as shown

Table 3. Electronic contribution of each atom.

InPS ₄					AlPS ₄					
Element	s	p	d	Total	ΔZ	Element	s	p	Total	ΔZ
S	1.89	4.52	0.00	6.41	-0.41	S	1.89	4.59	6.48	-0.48
P	1.46	2.85	0.00	4.30	+0.70	P	1.46	2.82	4.28	+0.72
In	0.96	1.11	9.99	12.06	+0.94	Al	0.76	1.02	1.78	+1.22

in Fig. 3. Most notable is the small difference between $\epsilon_1^{100}(\omega)$ and $\epsilon_1^{001}(\omega)$ which confirms the anisotropy and birefringence nature of the medium. This is best illustrated by the static limits of the calculated refractive indices of the compounds presented in Table 4 together with available experimental data. These values show a positive birefringence ($n_e(\omega) > n_o(\omega)$) for the uniaxial compound (InPS₄) which is in good agreement with the experimental data of Jantz *et al.* [10] (Fig. 4). We should emphasize that no experimental or previous theoretical data for AlPS₄ are available in the literature to make a meaningful comparison.

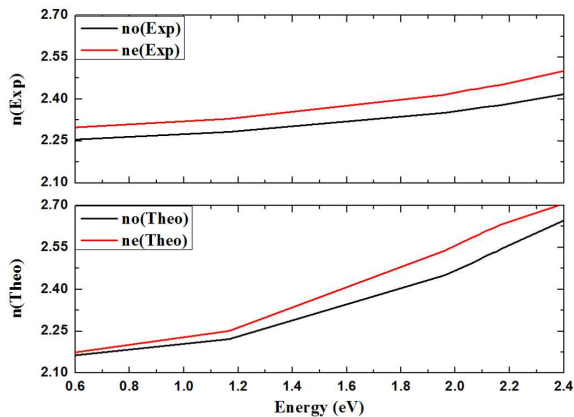


Fig. 4. Experimental and theoretical refractive indexes of InPS₄ in low frequency region.

3.3. Nonlinear optical properties

InPS₄ has four nonzero second order NLO tensor elements (d_{14} , d_{15} , d_{31} , d_{36}) imposed by the point group of the crystal and four electro-optic coefficients (r_{13} , r_{41} , r_{51} , r_{63}). Assuming Kleinmann symmetry conditions [35], these elements reduce to two independent elements $d_{14} = d_{36}$ and $d_{15} = d_{31}$. On the other hand, AlPS₄ second order NLO

tensor reduces to three non-vanishing elements ($d_{14} = d_{25} = d_{36}$).

The calculated NLO tensor elements d_{ij} and electro-optical coefficients r_{ij} are presented in Table 5. The calculated d_{ij} for InPS₄ are in fairly good agreement with the experimental counterparts with less than 10 % difference, whereas no experimental or theoretical data for AlPS₄ are available. Since our calculations procedures gave good results for InPS₄, we believe that NLO coefficients for AlPS₄ are reliable.

Regarding the electro-optic coefficients, to our knowledge no theoretical or experimental results have been published for these two materials. Therefore, our results show that InPS₄ is better candidate for electro-optic applications with higher E-O coefficients than AlPS₄. Nevertheless, we note that both compounds have low electro-optic coefficients compared to the standard ones.

3.4. Elastic and piezoelectric properties

The calculation of the piezoelectric tensors by Abinit code enabled us to evaluate four independent elements for InPS₄ and three for AlPS₄. These elements are presented in Table 6.

The calculated piezoelectric coefficients for InPS₄ are in good agreement with the experimental data except for d_{14} . Zhang *et al.* [36] explained this discrepancy by the fact that the piezoelectric coefficients are very sensitive to crystal quality, design of the samples and data processing method. On the other hand, these results show that AlPS₄ has higher piezoelectric coefficients than InPS₄ and better coefficients than reference materials such as quartz ($d_{14} = 0.727$ pC/N, $d_{11} = 2.310$ pC/N). It should be noted that no experimental or theoretical data are available to make a meaningful comparison.

Table 4. Refractive indices of InPS₄ and AIPS₄.

	InPS ₄			AIPS ₄		
	This work		Exp. [9]	This work		
	Castep (GGA)	Abinit (LDA)		Castep (GGA)	Abinit (LDA)	
Low ω (≈ 1.7 eV)						
$n_{(100)}(\omega)$	2.32	2.537	2.446	$n_{(100)}(\omega)$	2.07	2.135
$n_{(001)}(\omega)$	–	–	–	$n_{(001)}(\omega)$	2.07	2.176
$n_{(001)}(\omega)$	2.38	2.609	2.546	$n_{(001)}(\omega)$	1.95	2.114

Table 5. Electro-optic and second order optical coefficients of InPS₄ and AIPS₄ (in pm/V).

	InPS ₄		AIPS ₄	
	This work	Exp. [10]	This work	
d_{14}	31.54	28	d_{14}	-1.918
d_{15}	34.84	36	r_{41}	1.170
r_{13}	-4.12		r_{52}	0.620
r_{41}	-4.38		r_{63}	0.260
r_{51}	-3.99			
r_{63}	-4.13			

Table 6. Piezoelectric coefficients of InPS₄ and AIPS₄ (in pC/N).

	InPS ₄		AIPS ₄	
	This work	Exp. [8]	This work	
d_{14}	-1.16	8.7±1.5	d_{14}	-73.82
d_{15}	0.71	0.3±1.0	d_{25}	-10.69
d_{31}	6.73	-7.3±1.0	d_{36}	-28.19
d_{36}	12.58	21±1.5		

The calculated elastic coefficients of the compounds are presented in Table 7. It is clear that the calculated C_{ij} of InPS₄ are in good agreement with the available experimental data. Moreover, the elastic coefficients calculated by both the codes are very close. They also show that elastic coefficients of InPS₄ are twice smaller than those of quartz for both longitudinal and transverse elements. The elastic properties of AIPS₄ have not been reported in the literature yet. Since our calculations for InPS₄ gave good results, we believe that the present elastic coefficients for AIPS₄ can be taken as a reference for future investigations.

However, these theoretical results show that the compound (AIPS₄) has lower C_{33} as well as transverse coefficients compared to InPS₄. All stability criteria equation 7 and equation 8 are satisfied for both compounds except for Abinit calculated C_{66} of AIPS₄ that shows small negative value. As pointed out earlier and shown in Fig. 1, the one dimensional alternating AIS₄-PS₄ chains along x and y directions are hold together in the z direction by weak Van der Waals interactions. This configuration of atoms explains the high values of C_{11} and C_{22} and the small values of z oriented C_{33} , C_{66} coefficients. It also explains the unexpected negative values of C_{66} (Abinit) and C_{12} (Abinit) since Van der Waals interactions are not well accounted by standard DFT calculations. This is due to the fact they are long-range forces between fragments across lower density regions which are not accounted in local (LDA) or semi local (GGA) approximations of the exchange-correlation functional [37].

4. Conclusions

In summary, we have calculated the electronic structure, first and second order optical properties and electro-optical, elastic and piezoelectric tensors of the metal thiophosphates ternary compounds InPS₄ and AIPS₄ by means of density functional theory. The piezoelectric, electro-optic and second order optical tensors have been calculated using plane wave pseudopotentials method with local-density approximation (LDA) for exchange and correlation effects coupled with the modern theory of polarization. The calculated elastic constants, electro-optic, piezoelectric and second order

Table 7. Elastic constants of InPS₄ and AIPS₄ (GPa).

C _{ij}	InPS ₄				AIPS ₄		
	This work		Exp.		This work		
	CasteP LDA	Abinit LDA	Literature [9]	Literature [10]	C _{ij}	CasteP LDA	Abinit LDA
C ₁₁	44.15	44.03	43.80	43.68	C ₁₁	72.11	67.84
C ₃₃	39.58	39.44	40.70	40.56	C ₂₂	73.79	68.02
C ₄₄	23.41	21.97	22.80	22.80	C ₃₃	14.06	11.82
C ₆₆	16.52	15.78	13.60	13.92	C ₄₄	10.41	6.68
C ₁₂	8.98	10.31	8.90	9.02	C ₅₅	8.76	4.48
C ₁₃	25.22	25.55	26.60	23.80	C ₆₆	2.36	-1.46
C ₁₆	0.89	0.87	0.30	0.80	C ₁₂	0.54	-0.30
					C ₁₃	9.01	7.93
					C ₂₃	10.62	8.50

optical tensors of InPS₄ are in agreement with the available experimental results. Furthermore, these results show that AIPS₄ exhibits higher piezoelectric coefficient in comparison with quartz and is a promising candidate for piezoelectric applications.

Acknowledgements

The authors wish to thank the Laboratory of Physics of Materials funding this work. For the author A.H. Reshak the result was developed within the CENTEM Project, Reg. No. CZ.1.05/2.1.00/03.0088, co-funded by the ERDF as part of the Ministry of Education, the Youth and Sports OP RDI Program.

References

- [1] RICHARDSON K., CARDINAL T., RICHARDSON M., SCHULTE A., SEAL S., *Engineering glassy chalcogenide materials for integrated optics applications*, in: KOLOBOV A.V. (Ed.), *Photo-Induced Metastability in Amorphous Semiconductors*, Wiley-VCH Verlag GmbH & Co. KGaA, Weinheim, 2003, p. 383.
- [2] CHUNG I., KANATZIDIS M.G., *Chem. Mater.*, 1 (2014), 849.
- [3] VYSOCHANSKII Y.M., SLIVKA V.Y., CHEPUR D.V., *Quantum Electron.*, 20 (1981), 54.
- [4] LAVRENTYEVA A., GABRELIAN B.V., NIKIFOROV I.Y., REHR J.J., ANKUDINOV A.L., *J. Phys. Chem. Solids*, 8 (2003), 1251.
- [5] NITSCHKE R., WILD P., *Mater. Res. Bull.*, 6 (1970), 419.
- [6] CARPENTIER C.D., DIEHL R., NITSCHKE R., *Naturwissenschaften*, 8 (1970), 393.
- [7] BRIDENBAUGH P.M., *Mater. Res. Bull.*, 8 (1973), 1055.
- [8] BUBENZER A., NITSCHKE R., RAUFER A., *J. Cryst. Growth*, 3 (1975), 237.
- [9] HUARD F., EL HAIDOURI A., DURAND J., VACHER R., PELOUS J., *Mater. Res. Bull.*, 4 (1984), 415.
- [10] JANTZ W., KOIDL P., WETTLING W., *Appl. Phys. A-Mater.*, 2 (1983), 109.
- [11] BOLCATTO P.G., GRACIA E. A., SFERCO S. J., *Phys. Rev. B*, 24 (1994), 17432.
- [12] LAVRENTYEV A.A., GABRELIAN B.V., DUBEIKO V.A., NIKIFOROV I.Y., REHR J.J., *J. Phys. Chem. Solids*, 12 (2000), 2061.
- [13] LAVRENTYEV A.A., GABRELIAN B.V., NIKIFOROV I.Y., REHR J.J., ANKUDINOV A.L., *J. Phys. Chem. Solids*, 12 (2003), 2479.
- [14] LAVRENTYEV A.A., GABRELIAN B.V., KULAGIN B.B., NIKIFOROV I.Y., SOBOLEV V.V., *J. Phys. Chem. Solids*, 1 (2007), 315.
- [15] CLARK S.J., SEGALL M.D., PICKARD C.J., HASNIP P.J., PROBERT M.I.J., REFSON K., PAYNE M.C., *Z. Kristallogr.*, 5 – 6 (2005), 567.
- [16] HAMMER B., HANSEN L.B., NORSKOV J.K., *Phys. Rev. B*, 11 (1999), 7413.
- [17] VANDERBILT D., *Phys. Rev. B*, 11 (1990), 7892.
- [18] GONZE X., BEUKEN J.M., CARACAS R., DETRAUX F., FUCHS M., RIGNANESE G.M., SINDIC L., VERSTRAETE M., ZERAH G., JOLLET F., TORRENT M., ROY A., MIKAMI M., GHOSEZ P.H., RATY J.Y., ALLAN D.C., *Comp. Mater. Sci.*, 25 (2002), 478.
- [19] HAMANN D.R., WU X., RABE K.M., VANDERBILT D., *Phys. Rev. B*, 3 (2005), 035117.
- [20] ZHENG Y. SHI E., CHEN J., ZHANG T., SONG L., *J. Phys. Conf. Ser.*, 1 (2006), 61.
- [21] ZENG Y., ZHENG Y., XIN J., SHI E., *Comp. Mater. Sci.*, 56 (2012), 169.
- [22] LAGOUN B., BENTRIA T., BENTRIA B., *Comp. Mater. Sci.*, 68 (2013), 379.
- [23] TROULLIER N., MARTINS J.L., *Phys. Rev. B*, 3 (1991), 1993.
- [24] CEPERLEY D. M., ALDER B.J., *Phys. Rev. Lett.*, 7 (1980), 566.
- [25] PERDEW J.P., WANG Y., *Phys. Rev. B*, 23 (1992), 13244.
- [26] PERDEW J.P., BURKE K., ERNZERHAF M., *Phys. Rev. Lett.*, 18 (1996), 3865.
- [27] BASS M., *Handbook of Optics*, McGraw-Hill, New York, 1995.

- [28] NUNES R.W., VANDERBILT D., *Phys. Rev. Lett.*, 5 (1994), 712.
- [29] RESTA R., VANDERBILT D., *Theory of Polarization: A Modern Approach*, in: RABE K.M., AHN C.H., TRISCONE J.M. (Eds.), *Physics of Ferroelectrics*, Vol. 105, in: DRESSELHAUS M.S., LEE Y.P., OSSI P.M. (Eds.), *Topics in Applied Physics*, Springer, Berlin, 2007, p. 31.
- [30] VANDERBILT D., RESTA R., *Quantum Electrostatics of Insulators: Polarization, Wannier Functions, and Electric Fields*, in: LOUIE S.G., COHEN M.L. (Eds.), *Contemporary Concepts of Condensed Matter Science*, Elsevier, Amsterdam, 2006, p. 139.
- [31] NUNES R.W., GONZE X., *Phys. Rev. B*, 15 (2001), 155107.
- [32] VEITHEN M., GONZE X., GHOSEZ P., *Phys. Rev. B*, 12 (2005), 125107.
- [33] BAŘLON J.P., DORLOT J.M., *Des Materiaux*, Polytechnique, Montréal, 2000.
- [34] VANDERBILT D., *Systematic second-order perturbation theory for displacements, strains, and electric fields*, Rutgers University, New Brunswick, 2004.
- [35] KLEINMANN D.A., *Phys. Rev.*, 6 (1962), 1977.
- [36] ZHANG G., TAO X., WANG S., LIU G., SHI Q., JIANG M., *J. Cryst. Growth*, 1, (2011), 717.
- [37] LANGRETH D. C., DION M., RYDBERG H., SCHRODER E., HYLDGAARD P., LUNDQVIST B.I., *Int. J. Quantum. Chem.*, 5 (2005), 599.

Received 2015-05-04
Accepted 2016-04-29